

Supporting Information for

Hinokitiol potentiates antimicrobial activity of bismuth drugs: a combination therapy for overcoming antimicrobial resistance

Bacteria

The bacterial strains employed for antimicrobial and mechanistic studies are: *Staphylococcus aureus* (*S. aureus*) *S. aureus* USA600 (MRSA), *S. aureus* Mu3 (MRSA), *S. aureus* ST239 (MRSA), *S. aureus* 29213, *S. aureus* Newman, *Pseudomonas aeruginosa* (*P. aeruginosa*) PAO1, *P. aeruginosa* PA154197, *Escherichia coli* (*E. coli*) K12, *E. coli* V26 (NDM-1⁺), *Salmonella typhimurium* (*S. typhimurium*) 0839 (MCR-1⁺) and *Shigella flexneri* (*S. flexneri*) CH27 (MCR-1⁺) are from our own collection.

Chemicals

Colloidal bismuth citrate (CBS) was provided by Livzon Pharmaceutical Group. Hinokitiol was obtained from Energy. Kanamycin sulfate, Luria-Bertani (LB) Broth Powder, Mueller Hinton Broth (MHB), Brain Heart Infusion Broth (BHI) were purchased from Affymetrix. All other chemicals and reagents were from Sigma-Aldrich unless otherwise stated. All solvents used were purchased from ACI Labscan.

Cell lines

Lung cancer cell A549, human breast cancer cell MD-MBA-231 and glioma cell U251 purchased from American Type Culture Collection (Manassas, VA, USA) were cultured in Dulbecco's Modified Eagle's Medium (DMEM, Gibco, Grand Island, NY, USA) supplemented with 10% of Fetal Bovine Serum (FBS, Gibco Grand Island, NY, USA) and 1% of penicillin-streptomycin (Gibco BRL, Grand Island, NY, USA). Cells were maintained at 37°C, in an atmosphere of 5% CO₂ and 90% relative humidity.

Determination of MIC, MBC and FICI values

MIC (minimum inhibitory concentration) values were determined by broth micro-dilution method¹. Briefly, bacterial cells were cultured in LB or MHB broth at 37 °C on a culture shaker at 250 rpm. Cells grown to mid-log phase were diluted to 1×10⁶ CFU/mL with fresh medium and checked by CFU counting on agar pates afterwards. The tested compounds were 2-fold serial diluted into 96-well plates with a final volume of 50 μL bacterial suspension. The plates were then incubated at 37 °C for 20 ~ 22 hrs. The MIC was determined as the lowest concentration of a drug that could inhibit bacterial growth according to the measured OD₆₀₀ values.

At the end of MIC assay, aliquots of 50 μL tested solution from each well were plated to LB agar plates and incubated at 37 °C overnight. Resulting growth or lack of growth was examined after overnight culture and the lowest concentration that inhibits 99.9% of the original culture was taken as MBC (minimum bactericidal concentration) value.

For drug combination test, CBS and hinokitiol at the highest concentration of 128 μM were 2-fold serial diluted at different directions in 96 well plates. Other procedures were kept the same as MIC assay. The FICI (fractional inhibitory concentration index) is defined as the sum of the MIC of each drug when used in combination divided by the drug when used alone, i.e., $FICI = C_H/MIC_H + C_B/MIC_B$, where C_H and C_B are the concentrations of hinokitiol and Bi(III) at the effective combinations. Synergism was defined when FICI ≤ 0.5. All the determinations were performed in triplicate.

Cytotoxicity assay

About 4 × 10⁴ of A549, MDA-MB-231, U251 and HEPG2 cells were then exposed to various concentrations of Bi(III) and hinokitiol for 24 hrs. After a fixed incubation duration, 50 μL of XTT labeling mixture (Roche Diagnostics, USA) was added to each well, and the cells were incubated for 2 hrs at 37°C under a humidified atmosphere of 5% CO₂. The formation of formazan dyes, produced only by metabolic active cells, was detected spectrophotometrically at 490 nm. Measurements are performed in triplicate.

Time kill assay

S. aureus USA300 and *P. aeruginosa* PAO1 were cultured overnight and diluted 1:100 into MHB and LB broth at 37 °C for 3 hrs to reach log phase. The initial bacterial density was adjusted to $\sim 10^7$ CFU/mL and then exposed to hinokitol, Bi(III) either alone or in combination. Broth with no drugs served as a control. Aliquots of bacterial suspension were withdrawn at different time intervals (0, 1, 2, 4, 6, 8, 24 h) for inspection of bacterial viability by agar plating. The combinations of the drugs used in the test are 8 μ M for CBS, 24 μ M for hinokitol, and 8 μ M for Bi(Hino)₃. Data from three independent experiments were plotted as log₁₀ CFU/mL vs. time (h) for each time point over 24 hrs. All assays were triplicated and performed three times on different days.

Scanning electron microscopy

S. aureus Newman and *P. aeruginosa* PAO1 after the treatment of Bi(III) (50 μ M) or hinokitol (50 μ M) or their combinations for 4 hrs were collected and fixed in glutaraldehyde (2.5%) for at least 3 hrs and washed with phosphate buffered saline (PBS) for 4-6 times. The samples were subsequently exposed to ethanol dehydration series of 30%, 50%, 70%, 90% and 100% for 10 mins, and buffer exchanged to tertiary butanol. The samples were freeze-dried for 3 hrs, and sputter-coated with palladium-gold thin film. Images were recorded on a JSM-6330F (JEOL) field emission scanning electron microscopy.

Determination of anti-biofilm activity

S. aureus USA300 and *P. aeruginosa* PAO1 were used for anti-biofilm study. Colony biofilms were grown on UV-sterilized PE₂₀ urinary catheter. In brief, single colony of bacteria was inoculated in culture medium (BHI broth supplemented with 10% horse blood and 1% glucose for *S. aureus* and TSB broth supplemented with 0.5% glucose for *P. aeruginosa*) and incubated statically overnight at 37 °C. The overnight cultures were re-grown in fresh medium in a 1:5000 dilution. After two serial overnight passages, bacterial cells were inoculated into each well of a 24-well plate, 1 mL per well, in a 1:1000 dilution, in which Bi(III), hinokitol, or their combination were supplemented at various concentrations in respective well. Sterile PE₂₀ urinary catheter (0.58 mm \times 0.96 mm, coiled medical grade, UPS, USA) was cut into short tubes with 10 mm in length and allocated respectively into each well of 24-well plate containing as-prepared bacterial suspension. The plates were then incubated statically at 37 °C. After 48 h incubation, the catheters were collected from the bacterial suspension and gently washed three times with phosphate buffered saline (PBS) to remove the loosely adherent cells and planktonic cells, followed by air drying naturally. The biofilm growth was examined by measured the OD₅₄₀ nm for each well containing biofilm stain. To further quantify the production of biofilm, the catheters were prepared as above without staining in a separate experiment. Instead, each catheter was sonicated in aliquot of 500 μ L PBS for 5 min to disperse the biofilm, in which the bacterial loads on catheters were numerated by agar plating. Measurements were performed in triplicate.

Persister assay

S. aureus USA300 overnight culture was treated with 50 μ g/mL ciprofloxacin or 10 μ g/mL vancomycin for 4 h. After antibiotic treatment, cells were then washed three times with PBS and resuspended in PBS to give a concentration of 1.0×10^9 CFU/mL. 10 \times MIC of ciprofloxacin or vancomycin and 10 μ M CBS and 30 μ M hinokitol were added to the persister cells. The bacterial loads were numerated by agar plating on time points (0, 1, 2, 3, 4 hour). Measurements were performed in triplicate.

In vitro cell infection assay

About 2.0×10^5 A549 cells were seeded per well in 6-well plates and incubated for 48 hr to ensure confluency. Logarithmic cultures of *S. aureus* USA300 bacterial cells were washed with PBS for three times and re-suspended in culture medium resulting in the initial bacterial density of about 2.0×10^6 CFU/mL. Then, bacterial suspension was added to each well and substituted for the previous culture medium. The plates were centrifuged at 800 $\times g$ for 10 min and then incubated for another 1 h, executing the bacterial infection at multiplicity of infection (MOI) of 10.

Two infection models were used in this study, including the cell-associated bacterial infection and cell-invaded bacterial infection models. The cell-associated bacteria are herein defined as bacteria that attach to, penetrate, or transcytose in A549 cells, while the cell-invaded bacteria are defined as bacteria that penetrate or transcytose A549 cells. For the cell-invaded infection, the infected cells were incubated in culture medium supplemented with gentamicin (400 $\mu\text{g}/\text{mL}$) for 1 h to remove extracellular bacteria. Then, the treated cells were washed vigorously with PBS for six times and replenished with culture medium. For the cell-associated infection, the infected cells were only washed vigorously with PBS for six times to remove unbound bacteria. The infected A549 cells were then exposed to either CBS or hinokitiol, or their combination overnight under identical cell culture conditions. Cells in the absence of drugs served as a control. The bacterial loads were examined by lysing A549 cells with 1% Triton X-100 in PBS and serially diluting the resulting lysates to enumerate bacterial colonies by agar plating. The assay was performed in triplicate, repeated three times, and results were expressed as average \pm SD.

UV-vis spectroscopy

UV-vis spectroscopic titration was carried out on a Varian Cary 50 spectrophotometer at a rate of 360 nm min^{-1} using a 1-cm quartz cuvette at 25 $^{\circ}\text{C}$. For the stoichiometry of Bi^{3+} binding to hinokitiol, appropriate amounts of 100 μM CBS stock solution were added to a 1-mL aliquot of 100 μM hinokitiol in titration buffer (20 mM Tris-HCl, pH 5.2) to generate varying molar ratios of Bi^{3+} to hinokitiol. The samples were left 3 mins between each detection. The absorbance at 380 nm was recorded. The stoichiometry of Bi-hinokitiol was estimated from the titration curve.

Measurement of Fe(III) uptake

Bacterial cells were incubated overnight in iron-depleted cation-adjusted Mueller-Hinton broth (ID-CAMHB), which was prepared by Mueller-Hinton broth treated with cation binding resin Chelex 100, followed by the supplement of Ca^{2+} , Mg^{2+} and Zn^{2+} to maintain bacterial growth. Later, 5 μM of fluorescent intracellular iron indicator calcein-acetoxymethyl (calcein-AM) was added while 1.5 μM of chloramphenicol was added to restrain cell activity. The cells were washed with PBS after 3 hrs of light-shielded incubation at room temperature, adjusted to $\text{OD}_{600} = 0.5$, supplemented with 10 μM ammonium iron citrate and transferred to 96-well plate immediately. The fluorescence intensity was observed with 492 nm excitation and 535 nm emission by SpectraMax iD3 (Molecular Devices, CA). After 90 s monitoring, CBS (400 μM), hinokitiol (60 μM) and their combinations were added. The fluorescence was monitored for another 210s.

Measurement of Bi(III) uptake

Bacterial cells were harvested after 30 mins and 180 mins treatment with or without 50 μM or 150 μM of hinokitiol. After washing with cold PBS containing 5 mM EDTA, cell pellets were digested with 70% HNO_3 (trace metal basis, Sigma) at 60 $^{\circ}\text{C}$ overnight. Samples were diluted by *ca.* 5% HNO_3 to a final concentration and analyzed by ICP-MS (iCAP RQ, Thermo Fisher).

Thermal proteome profiling

S. aureus USA300 was treated with vehicle (solution without the drug), 300 μM CBS, 300 μM hinokitiol or their combinations for 2 hours in biological duplicates. The cells were washed by ice-cold PBS twice and then resuspended in 2mL lysis buffer (25 U/mL OmniNuclease, 50 $\mu\text{g}/\text{mL}$ lysozyme, 2mM MgCl_2 in PBS). The enzymes were allowed to activate for 20 min. The cells were then lysed via sonication at the amplitude of 26% on ice-water bath (5 s on, 10 s off, in total 20 min). The sonicated cells were then centrifuged at 15,000 rpm for 10 min to separate the lysate from cell debris. The cell lysates were transferred into 0.2 mL PCR tubes, followed by heating each tube in parallel in a thermal cycler machine from 37 to 80 $^{\circ}\text{C}$ for 3 min. The cell lysates were then centrifuged at 15,000 rpm for 10 min to obtain the soluble proteins.

For each sample, add 8M urea/100 mM Tris-HCl solution (pH=8.5) to 50 μg protein to make the final concentration of urea around 6 M, followed by denaturing at 60 $^{\circ}\text{C}$ for 10 min. Then, the protein sample was reduced with 10mM dithiothreitol (DTT) for 20min at room temperature and alkylated with 25mM iodoacetamide (IAA) in the dark for 30min at room temperature. Before adding trypsin at a ratio of 1:50 to

digest for 16 h at 37°C, the alkylated sample was diluted with 100mM Tris-HCl buffer pH 8.5 to the final concentration of 1M urea. Acidify the reaction by adding the formic acid to 5% (v/v), and the insoluble material was removed by centrifugating at 14,000 rpm for 15 min. Samples were desalted using in-house-made C18 stage tips and then speed-vacuum to completely dry².

For each sample, 25µg dried peptides were dissolved with 25µL 50mM TEAB (pH=8.5). 41µL acetonitrile was added to each TMT reagent and occasional vortexing for 5 min. 10.25 µL TMT reagent was carefully added to each redissolved sample and incubated for 1 h at room temperature. The reaction was quenched by adding 5% hydroxylamine to 0.4% (v/v) for 15 min. The labeled samples were combined into a new microtubes and then adjust the acetonitrile < 5% by adding 0.1% formic acid. Use the C18 stage tips to desalt the samples for LC-MS/MS analysis.

LC-MS/MS analysis was performed on an Orbitrap Fusion Tribrid mass spectrometer (Thermo-Scientific) with a Easyspray ion source (Thermo-Scientific) connected to an Easy-nLC 1200 system (Thermo-Scientific) with a 50-cm Easyspray column. The mobile phases consisted of buffer A (0.1% formic acid) and buffer B (0.1% formic acid in 80% ACN). TMT labeled samples were resuspended in buffer A and introduced through the autosampler of the Easy-nLC 1200 system. Peptides were eluted, further separated by a 245 min gradient from 8% to 38% B followed by a 25min column wash-off to 100% B at a flow rate of 300 nL/minute and sprayed directly into the MS. Positive ion mode was applied with a voltage of 1800 V and a transfer tube temperature of 275°C. Data-dependent acquisition (DDA) was applied. The Full scans were recorded at a resolution of 60K with a mass range from 375 to 1500 m/z. The HCD MS/MS was performed with quadrupole isolation mode, 0.7 Da isolation window, 38% collision energy and recorded at a resolution of 30 K.

The raw data files were processed by Proteome Discoverer (version 2.5, Thermo Fisher Scientific). The data were searched against protein database of *S. aureus* USA300 from Uniprot (downloaded on 26 March 2024, 6576 entries) by using Sequest. The following parameters were used for protein identification, peptide mass tolerance of 10 ppm; MS/MS tolerance of 0.6 Da; enzyme was trypsin, missed cleavage of 2; fixed modification, carbamidomethyl (C), TMT10-plex (K) and TMT10-plex (N-term); variable modification, and oxidation (M). Protein false discovery rate was set as 0.01. The intensities of TMT reporter ions in the MS/MS spectra were calculated for quantification.

The statistical analysis of TPP data was performed by using TPP package⁶³. The intensities of reporter ions were firstly scaled based on the lowest temperature (37°C). The ΔT_m fitting and non-parametric analysis of response curves (NPARC) fitting were utilized to screening the potential drug targets (*SI Appendix*, Fig. S4).

For ΔT_m fitting, the relative intensities were fitted as a sigmoidal trend with the following equation:

$$f(T) = \frac{1 - plateau}{1 + e^{-\frac{a}{T} - b}} + plateau$$

Where T is the temperature and a, b, and plateau are constants. The melting point T_m value is defined as half of the protein amount has been denatured. The slope of the melting curve is defined as the value of the first derivative of $f(T)$. The quality of fitting was evaluated based on (A) both fitted melting curves have a coefficient of determination $R^2 > 0.8$; (B) the two curves from diverse replicates have a plateau < 0.35 ; (C) the slope of the melting curve < -0.06 ; (D) the difference of T_m in two replications < 2.5 .

For NPARC fitting, the relative intensities were fitted as a stochastic process with a smooth mean function, and then constructs its hypothesis tests directly on these samples. The p-values were calculated based on the F-statistic which uses a more flexible model that makes fewer assumptions on the data than ΔT_m fitting.

The proteins with $\Delta T_m > 2.5$ in ΔT_m fitting and Benjamini-Hochberg adjusted p-values < 0.05 were selected as potential drug targets. Density plot was applied to reveal the distribution of the T_m before and after drug treated³. The volcano plot was utilized to virtualize the selection of potential drug targets⁴.

GO enrichment analysis was performed using STRING 12.0 against *S. aureus*⁵. The protein-protein-integration network with highest confidence (>0.900) from experiments or curated databases was export and virtualized in Cytoscape^{6,7}.

Proteomics analysis

S. aureus USA300 was treated with vehicle (solution without the drug) and the combination of 300 μ M CBS and 300 μ M hinokitil for 2 hours in biological triplicates. The cells were collected at different time intervals (0.5, 1, 2 and 4 h) and washed by ice-cold PBS twice and then resuspended in 1 mL lysis buffer (6 M urea, 25 U/mL OmniNuclease, 50 μ g/mL lysozyme, 2 mM $MgCl_2$ in PBS). The enzymes were allowed to activate for 20 min. The cells were then lysed via sonication at the amplitude of 26% on ice-water bath (5s on, 10s off, in total 20 min). The sonicated cells were then centrifuged at 15,000 rpm for 10 min to separate the lysate from cell debris.

For each sample, 50 μ g protein was precipitated by adding 6x volume of $-20^\circ C$ acetone (gr grade, Duksan) to ice-cold sample. Vortex well and keep at $-20^\circ C$ overnight. After that, spin the microtubes in 12,000 g for 20 min and then remove supernatant, followed by air dry the pellet. Later, acetone-precipitated proteins were dissolved in 50 μ L 8M urea/100 mM Tris-HCl solution (pH=8.5), followed by denaturing at $60^\circ C$ for 10 min. Then, the protein sample was reduced with 10 mM DTT for 20 min at room temperature and alkylated with 25mM IAA in the dark for 30min at room temperature. Before adding trypsin at a ratio of 1:50 to digest for 16 h at $37^\circ C$, the alkylated sample was diluted with 100mM Tris-HCl buffer pH 8.5 to the final concentration of 1M urea. Acidify the reaction by adding the formic acid to 5% (v/v), and the insoluble material was removed by centrifugating at 14,000 rpm for 15 min. Samples were desalted using in-house-made C18 stage tips and then speed-vacuum to completely dry².

For each sample, 25 μ g dried peptides were dissolved with 25 μ L 50mM TEAB (pH=8.5). 41 μ L acetonitrile was added to each TMT reagent and occasional vortexing for 5 mins. 10.25 μ L TMT reagent was carefully added to each redissolved sample and incubated for 1 h at room temperature. The reaction was quenched by adding 5% hydroxylamine to 0.4% (v/v) for 15 min. The labeled samples were combined into a new microtubes and then adjust the acetonitrile $< 5\%$ by adding 0.1% formic acid. Use the C18 stage tips to desalt the samples for LC-MS/MS analysis. For the LC-MS/MS analysis and raw data processing, the procedures are same as described in Thermal proteome profiling.

To minimize the batch effect due to the TMT reagents, internal reference scaling normalization was applied⁸. The differentially expressed proteins (DEPs) were screened by using MetaboAnalyst and based on the p-value < 0.05 in two-sample t-test and fold change of protein abundance > 1.2 ⁹. The overrepresented biological processes within communities were enriched by using STRING.

Topology analysis was performed to predict the drug targets based on betweenness and degree by NetworkAnalyzer¹⁰. In a binary network with n nodes (where each node represents a gene), the total degree centrality of a node i (d_i) is defined as the total number of direct connections (or linkages) it has with other nodes in the network. Mathematically, this is expressed as:

$$d_i = \sum_{j=1}^n a_{ij}$$

where a_{ij} is 1 if there is a linkage between nodes i and j , and 0 otherwise. Degree centrality is a straightforward measure that only considers the local impact of a node through its direct connections. However, it does not account for nodes that, despite having few connections, are crucial connectors within the network. This is where betweenness centrality becomes useful.

Betweenness centrality measures the importance of a node based on the number of shortest paths that pass through it. For a node i , the betweenness centrality b_i is calculated as:

$$b_i = \sum_{s \neq i \neq t} \frac{P_{st(i)}}{P_{st}}$$

Where P_{st} is the total number of shortest paths between nodes s and t , and $P_{st(i)}$ is the number of those paths that pass-through node i . Betweenness centrality captures the global importance of a node by considering both its direct and indirect connections, making it effective in identifying key connectors or bottlenecks in a network.

RNA extraction and qRT-PCR

The total RNAs of *S. aureus* were extracted using MiniBEST Universal RNA Extraction Kit (TaKaRa) according to the protocol. The extracted RNA samples were subjected to DNase I treatment to completely remove contaminated genomic DNA. The quantity of RNA were determined by NanoDrop 2000 (Thermo Fisher Scientific). PrimeScript RT Master Mix (Perfect Real Time) (TaKaRa) was used for reverse transcription. Real-time PCR reactions were performed on StepOnePlus Real-Time PCR system (ABI) with TB Green Premix Ex Taq II (TaKaRa). $\Delta\Delta C_T$ method was utilized to quantify the transcription level of target genes and the levels were normalized to the house-keeping gene *16s*. Each sample was assessed in three biological replicates. The primers used for qRT-PCR are listed in Table S4.

***In vivo* bismuth content studies**

All animal related experiments were approved by, and performed in accordance with the guidelines approved by Committee on the Use of Live Animals in Teaching and Research (CULATR) of the University of Hong Kong. For all of mouse experiments, 6-to-8-week-old female BALB/c mice with body weight of 18-22 g, were purchased from Charles River Laboratories, Inc. All animal procedures were approved by CULATR of the University of Hong Kong (reference code: CULATR 22-176). All the animals were randomly caged in biosafety level housing and given access to standard pellet feed and water ad libitum before the commence of corresponding experiments.

To estimate the impact of hinokitiol on blood bismuth content, groups of mice ($n= 5$ per group) were administered with CBS (100 mg/kg), CBS (100 mg/kg) + hinokitiol (120 mg/kg) via oral gauge, respectively. Mice were sacrificed at 0.5, 1, 2, 4, 8 and 24-hour post-dosing and $\sim 600 \mu\text{L}$ of blood per mouse were drawn in heparinized centrifuge tubes. Blood was acidified with HNO_3 and subjected to ICP-MS for bismuth content measurement. Blood from untreated mice was collected and used as a control to estimate matrix effects.

For the measurement of bismuth accumulation in mouse lung, kidney, spleen and liver, groups of mice ($n= 5$ per group) were orally administrated with CBS (100 mg/kg) and CBS (100 mg/kg) + hinokitiol (120 mg/kg). The mice were sacrificed after 2, 24 and 48 hours and the organ tissues were dissected after cardiac perfusion with 0.9% saline, and acidified with 69% HNO_3 for the measurement of bismuth content by using ICP-MS.

Mouse wound infection model

The mouse wound infection model was modified based on a previously described method¹¹. The right flanks (infection sites) of the mice were shaved and the skin was sterilized with iodine solution and 75% ethanol to the bacterial infection on Day 0. All the mice were anesthetized with Ketamine-Xylazine combination (Ketamine: 100 mg/kg, Xylazine: 10 mg/kg, Aldamedics) for pain management, A 6.0-mm disposable skin biopsy punch (Biopunch, Inc.) was used to generate a full-thickness skin defect overlying the thoracic spinal column and the adjacent musculature. Then, a 20- μL aliquot containing 1×10^7 CFU of log-phased *S. aureus*, was pipetted over the wound. Then, these wounds were directly treated with 20 μL vehicle (cream), CBS (2 mg/kg, cream) + hinokitiol (2.5 mg/kg, cream) and CBS (10 mg/kg) + hinokitiol (25 mg/kg, cream), respectively (Day 1) and once daily thereafter. On Day 7, all wound beds were collected, homogenized and

the corresponding bacterial loads were numerated by agar plating. Body weight as well as health status was monitored until the end of experimental period.

Mouse gastrointestinal infection model

All mice were administered with antibiotic cocktail (50 mg/kg ampicillin, 50 mg/kg metronidazole, 50 mg/kg neomycin, 50 mg/kg vancomycin) once daily for consecutive 7 days and cease 3 days prior to infection. During the period, feces were collected for CFU checking on mannitol salt agar. *S. aureus* USA300 were grown to mid-exponential growth phase, washed and resuspend in PBS. Mice were inoculated by oral gauge with 200 μ L of 2×10^8 CFU/mL USA300 suspension. 100 mg/kg CBS, 120 mg/kg hinokitiol and their combination were given once a day for 4 consecutive days. Mice were sacrificed on Day 5. Feces were collected and weighed. Intestinal colonization was evaluated by quantitative cultures of mouse feces and small intestine on mannitol salt agar.

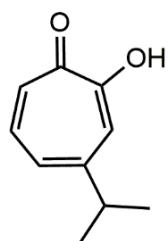
Mouse bloodstream infection model

S. aureus USA300 were cultured in MHB overnight at 37°C with 250 rpm shaking and diluted 1:100 to reach $OD_{600}=3$, then the bacterial pellets were collected, washed with PBS and diluted to 2×10^8 CFU/mL. The groups of mice ($n= 30$ per group) were first infected by *S. aureus* through i.v. injection of 100 μ L USA300 suspension, then were orally administered with CBS (50 mg/kg), hinokitiol (60 mg/kg) and CBS (50 mg/kg) + hinokitiol (60 mg/kg) at 30 mins post infection and for 4 consecutive days. All mice were sacrificed on Day 5 post infection and their weighed livers, lungs, kidneys and spleens were placed into 1 mL sterile PBS on ice, and then homogenized to numerate bacterial loading by agar plating. Body weight as well as the health status of mice was monitored until the end of experimental period.

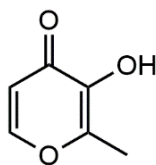
Animal toxicity and histology studies

Toxicity experiments were conducted with BALB/c mice. CBS (100 mg/kg) and hinokitiol (120 mg/kg) were administered once daily for consecutive 7 days and sacrificed 24 hrs after the whole dose regimen. 5 mice were used for each group and mice receiving vehicle served as control. The body weight of mice was monitored once daily. For plasma ALT, BUN and creatinine assay, all the mice were sacrificed on day 8, plasma and serum of mice was collected and subjected to the assay according to the manufacturer's instruction.

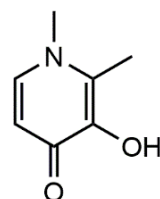
Samples of mouse lung, brain, liver, spleen and kidney were collected for histological examination. The tissue sections were mounted on glass slides and subjected to routine staining with hematoxylin and eosin (HE) method. The HE-stained sections were subsequently examined under a light microscope to identify any abnormal histopathological characteristics.



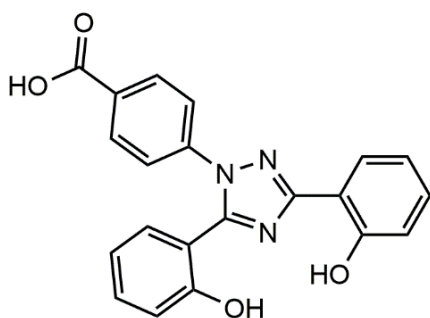
Hinokitiol



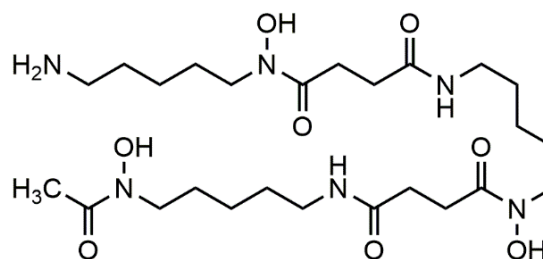
Maltol



Deferiprone



Deferasirox



Deferoxamine

Fig. S1. Chemical structures of metal-chelating ligands used in this study.

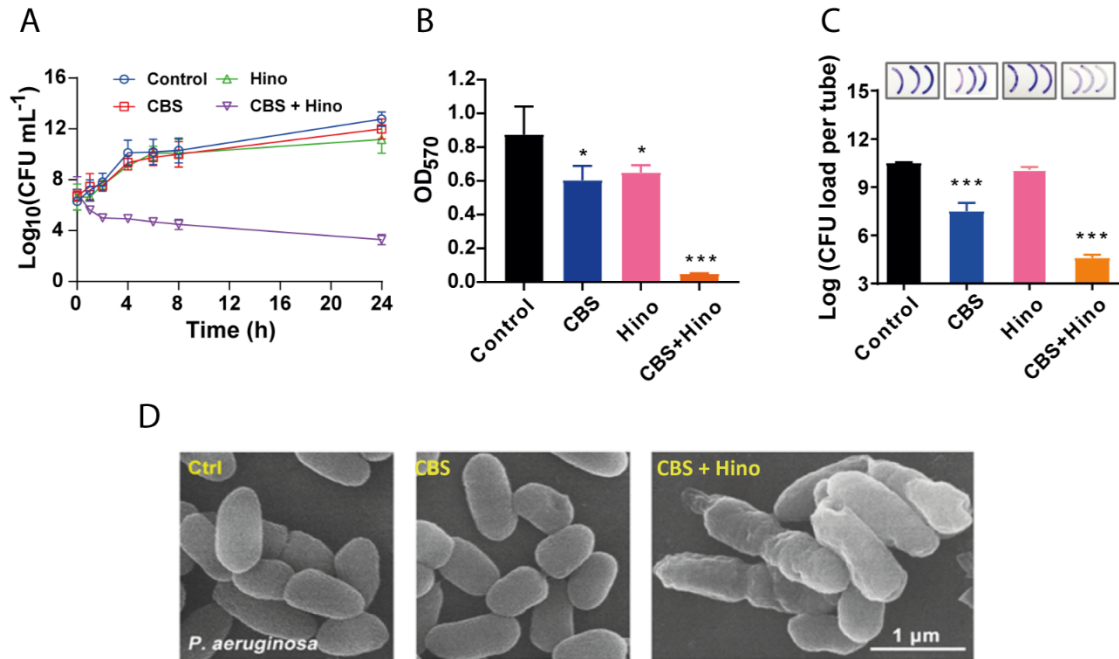


Fig S2. (A) Time-kill curves for CBS and hinokitiol monotherapy and combination therapy against *P. aeruginosa* PAO1. (b) Bar charts showing the bacterial loads of pre-formed biofilm by *P. aeruginosa*. (c) The degree of biofilm formation when *P. aeruginosa* were exposed to treatment of compounds prior to the formation of biofilm. The insets show the crystal violet-stained image of the catheter treated with vehicle control, combination of CBS and hinokitiol or single component. (d) Scanning electron microscope (SEM) images of *P. aeruginosa* show destroyed morphology of bacteria treated with the combination of Bi(III) (50 μM) and hinokitiol (50 μM).

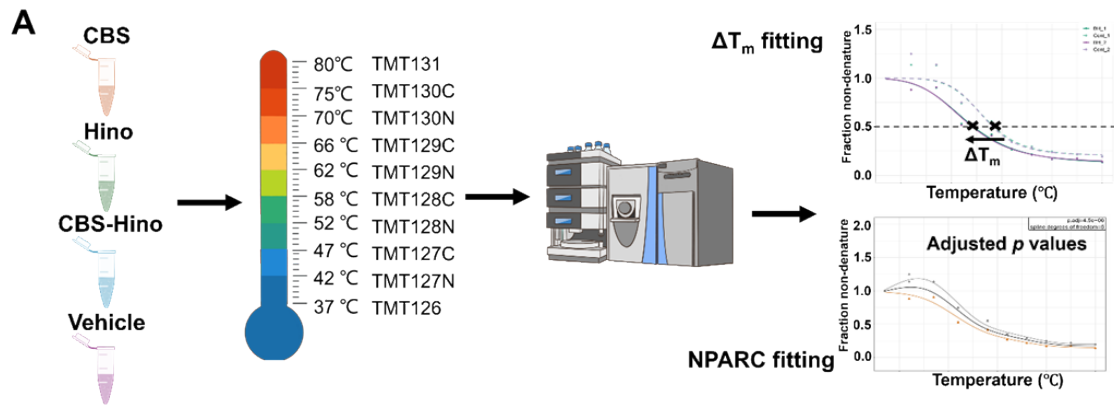
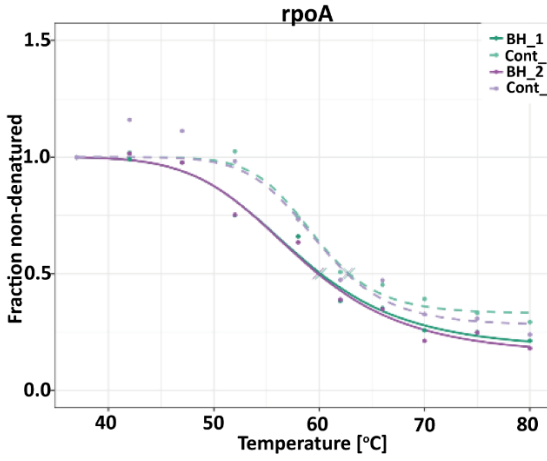
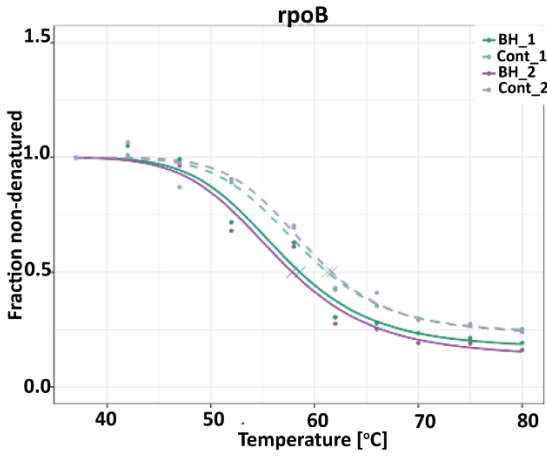
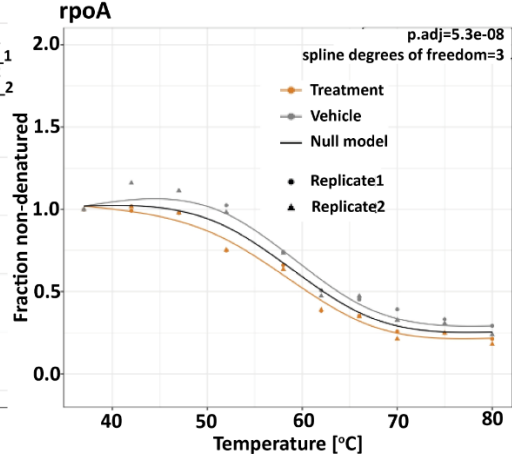


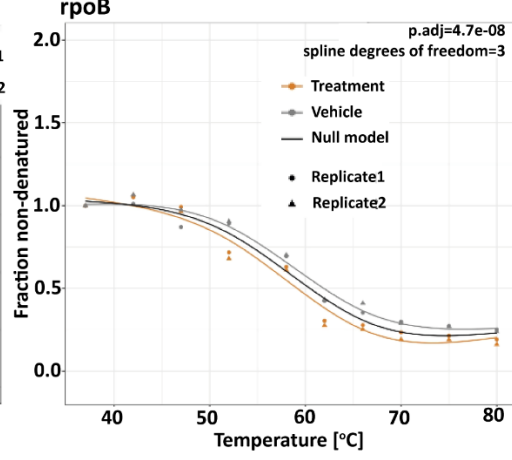
Fig. S3. Schematic plot of the TPP experiment.



	meltPoint	slope	plateau	R2
BH_1	60.14	-0.041	0.71	0.98
Cont_1	62.86	-0.057	0.33	0.99
BH_2	59.89	-0.042	0.15	0.99
Cont_2	62.64	-0.055	0.28	0.95



	meltPoint	slope	plateau	R2
BH_1	58.58	-0.048	0.17	0.97
Cont_1	61.23	-0.047	0.23	0.98
BH_2	57.86	-0.048	0.13	0.97
Cont_2	61.66	-0.05	0.24	0.99



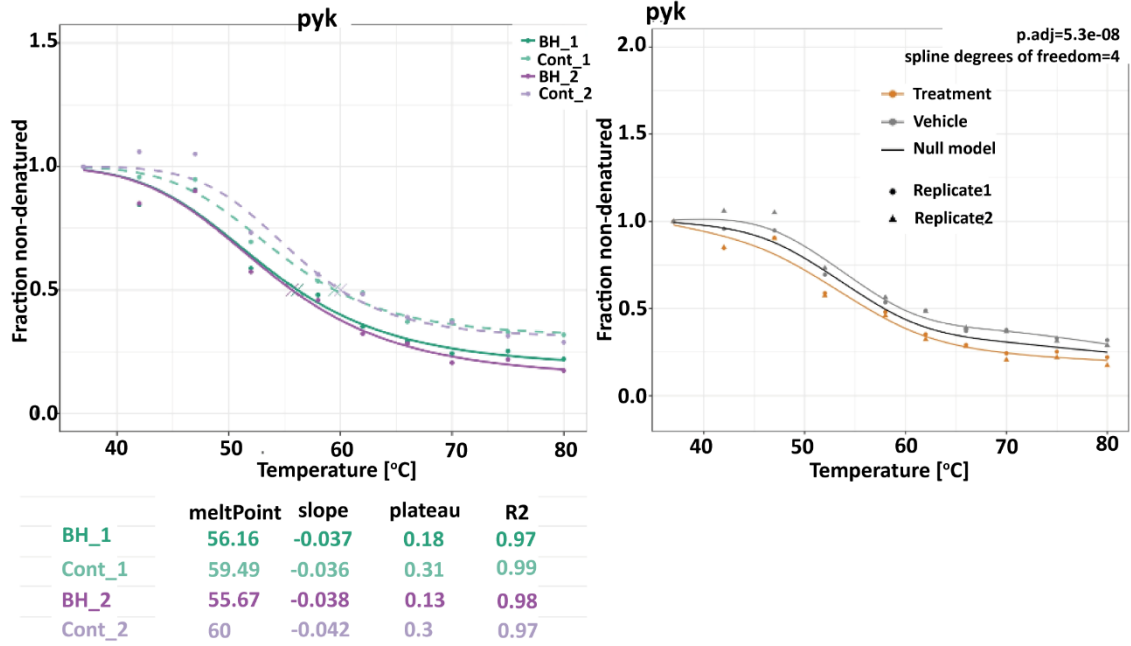


Fig. S4. The ΔT_m fitting and NPARC fitting for *rpoA*, *rpoB* and *pyk*.

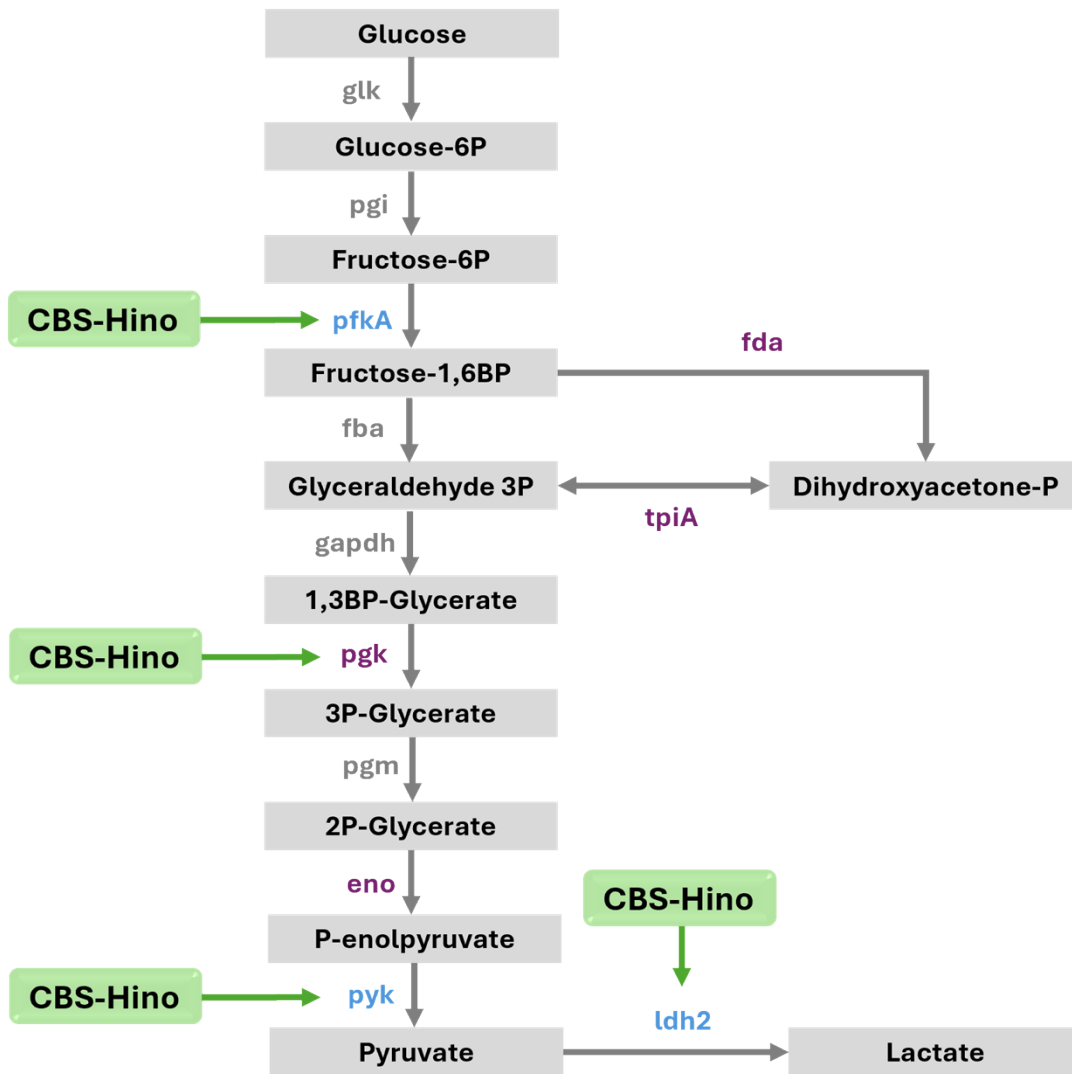
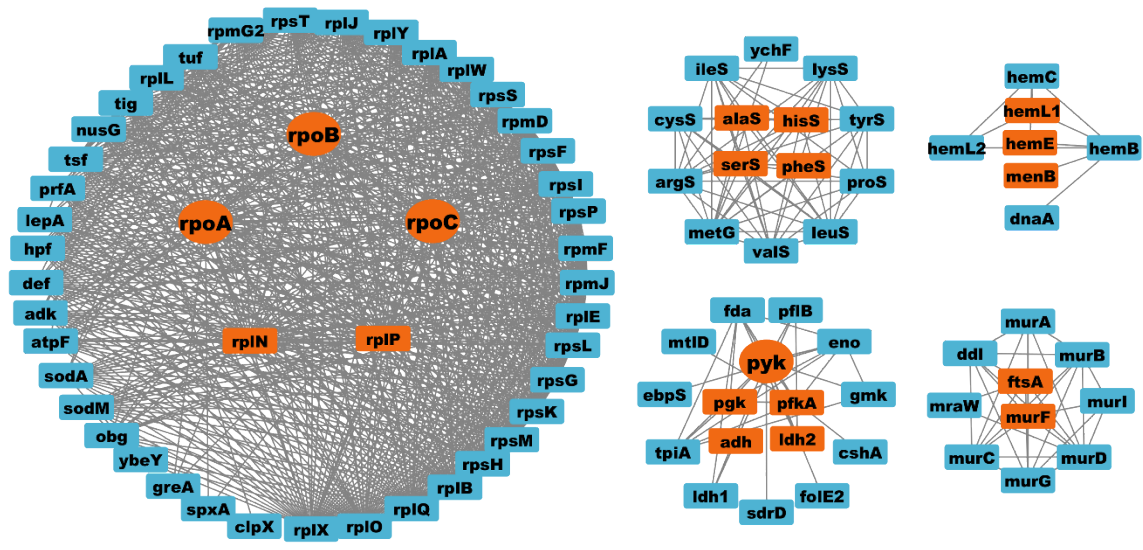


Fig. S5. Diagram showing the identified CBS + hinokitiol targeting proteins in glycolytic pathway and how bismuth-hinokitiol disrupts glycolysis in *S. aureus*.



Cluster	Biological pathway	Ratio	FDR
①	Translation	0.31	7.69e-30
①	Transcription, DNA-templated	0.31	6.00e-04
②	tRNA aminoacylation for protein translation	0.65	7.35e-23
③	Protoporphyrinogen IX biosynthetic process	0.71	1.48e-08
④	Glycolytic process	0.53	1.47e-11
⑤	Peptidoglycan biosynthetic process	0.33	1.28e-11

Fig. S6. PPI network among DEPs (blue) and TPP hits (orange). Markov clustering algorithm (MCL) was applied to detect the functional clusters. The enlarged balls (*rpoA*, *rpoB*, *rpoC* and *pyk*) are hub nodes identified by topology analysis with the largest betweenness and degree among all the TPP hits in the network.

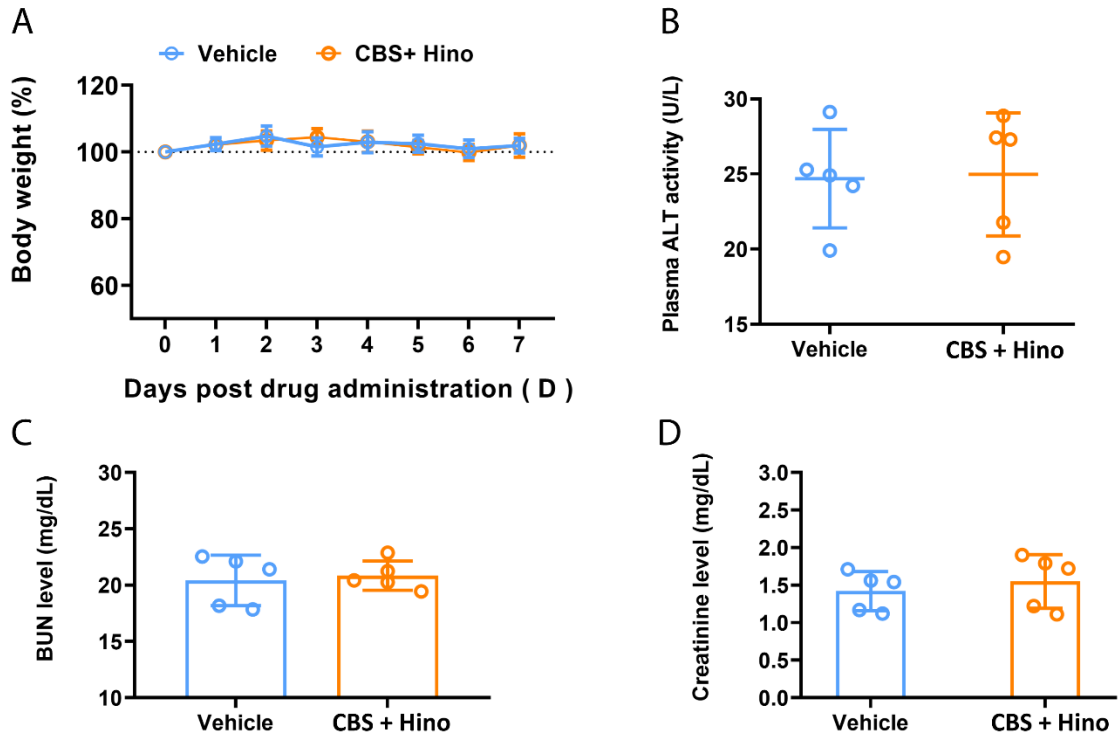


Fig. S7. Toxicological studies of BALB/c mice received CBS + hinokitiol for consecutive 7 days compared to vehicle group (PBS). Toxicity studies were done using 5 mice per group. (A) The body weight change of mice after drug treatment. (B) The biomarker plasma levels of ALT in groups of mice received vehicle control versus CBS + hinokitiol cotreatment. (C) BUN level and (D) creatinine level of mice treated versus untreated with CBS + hinokitiol.

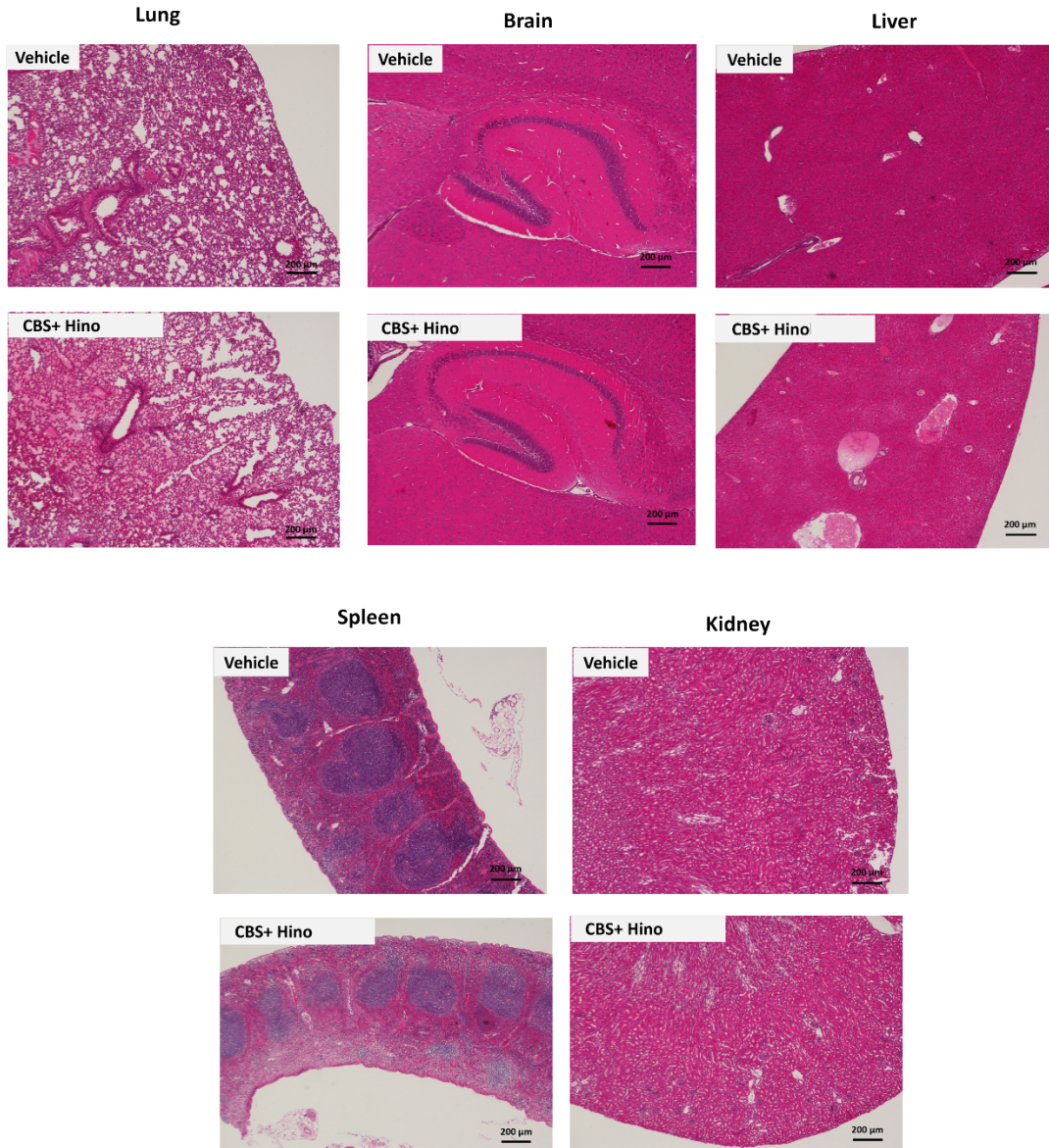


Fig. S8. Hematoxylin and eosin (H&E) staining of the mouse lung, brain, liver, spleen and kidney tissue sections from vehicle control and CBS + hinokitiol groups post drug treatment for consecutive 7 days. Experiments were performed in triplicate. Scale bar: 200 µm.

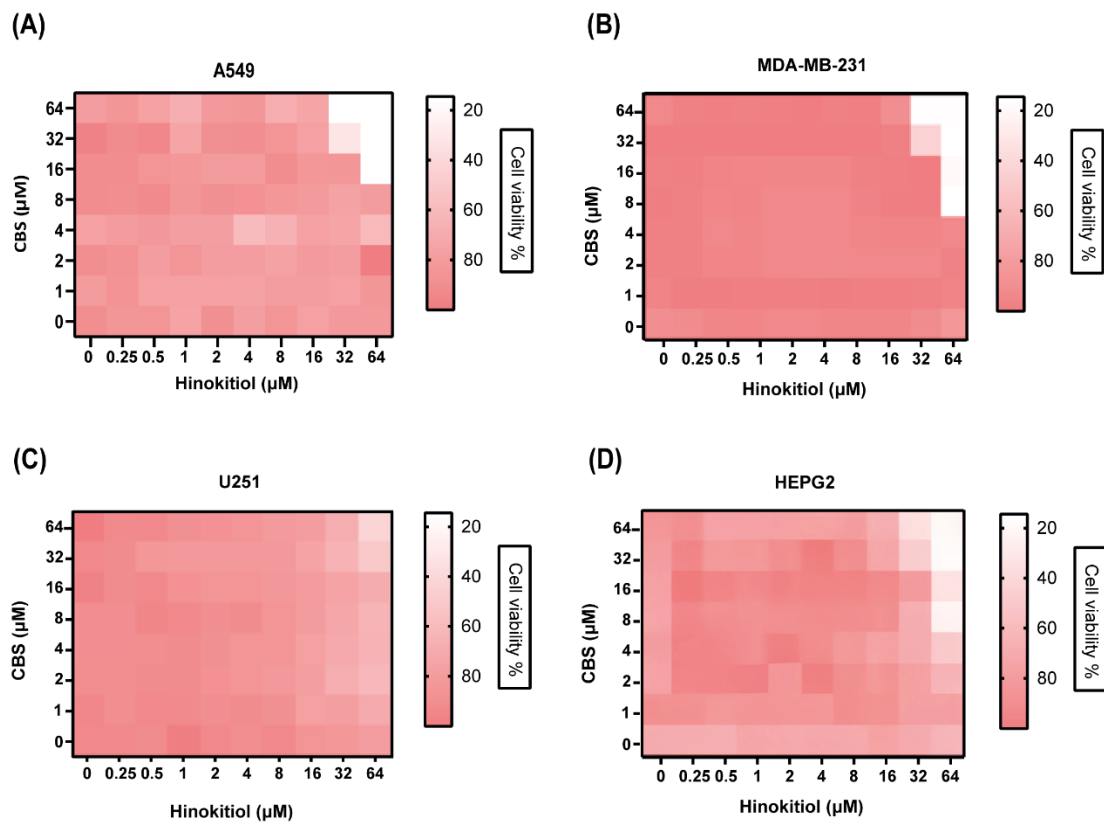


Fig. S9. Cytotoxicity assay of the combination of CBS and hinokitiol in (A) A549, (B) MDA-MB-231, (C) U251 and (D) HepG2 cell.

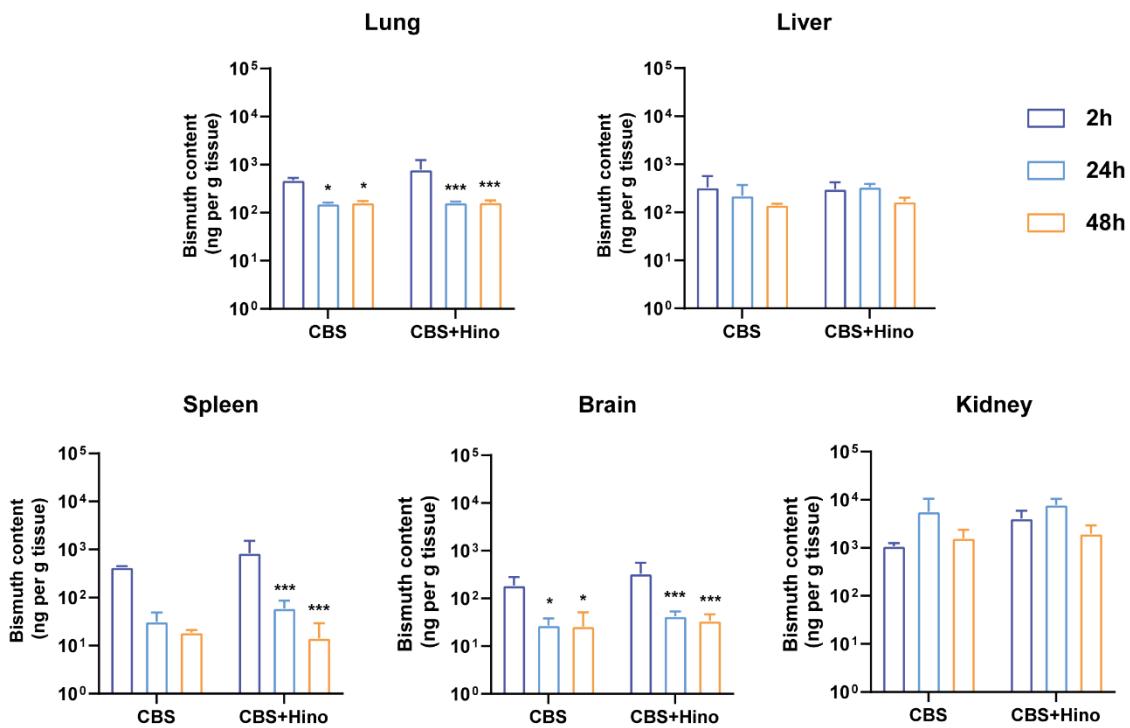


Fig. S10. Bismuth distribution in lung, liver, spleen, brain and kidney after oral administration of CBS (100 mg/kg) and CBS+3x hinokitiol in mice (n=5) for 2, 24 and 48 hours. Statistical significances were determined using ANOVA, ***p<0.001, ** p<0.01, *p<0.05.

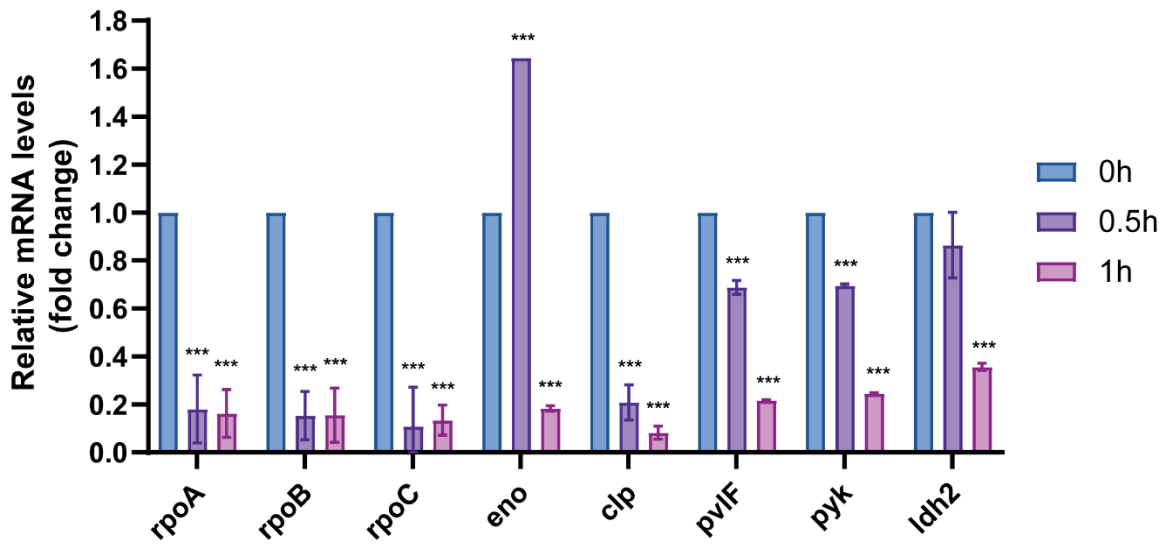


Fig. S11. Relative mRNA expression levels were assessed by qPCR. Gene expression levels were measured at 0 (baseline), 0.5 and 1 hour post-treatment and normalized against *16s*. Statistical significances were determined using ANOVA, *** $p < 0.001$, ** $p < 0.01$, * $p < 0.05$.

Table S1. Minimum inhibition concentration/ Minimum bactericidal concentration (μM) of laboratory and clinical isolated bacteria to Bi(III) or Ga(III), and their combination with metal-chelating ligands. Hino stands for hinokitiol.

Compounds	<i>S. aureus</i>	<i>P. aeruginosa</i>	<i>E. coli</i> K12	<i>B. cenocepacia</i> J2315
	Newman	PAO1		
Bi(NO ₃) ₃	>256	32/ >256	>256	32/ >256
Bi(NO ₃) ₃ + Hino	2/8	4/16	32/128	16/ >256
Bi(Hino) ₃	8/16	8/32	32/64	32/64
Bi(NO ₃) ₃ + Deferiprone	>256	64/ >256	>256	64/ >256
Bi(DFP) ₂	>256	64/ >256	>256	64/ >256
Bi(NO ₃) ₃ + Maltol	>256	32/ >256	>256	64/ >256
Bi(Mal) ₂	128/ >128	32/256	>256	32/256
Bi(NO ₃) ₃ + Deferoxamine	256/ >256	32/ >256	>256	32/ >256
Bi(NO ₃) ₃ + Deferasirox	256/ >256	16/ >256	>256	16/ >256
Ga(NO ₃) ₃	256/ >256	64/ >256	>256	
Ga(NO ₃) ₃ + Hino	256/ >256	128/ >256	>256	
Ga(NO ₃) ₃ + Deferiprone	256/ >256	256/ >256	>256	
Ga(NO ₃) ₃ + Maltol	256/ >256	256/ >256	>256	
Ga(NO ₃) ₃ + Deferoxamine	256/ >256	256/ >256	>256	
Ga(NO ₃) ₃ + Deferasirox	256/ >256			

*Bismuth nitrate dissolved in 50% glycerol (10 mM stock solution) was used in the assay. The ligands are dissolved in DMSO/H₂O with a final concentration of 50 μM . The MIC values of the ligands to all bacteria are > 256 μM .

Table S2. Thermal protein profiling for *S. aureus* upon the combined CBS and hinokitiol treatment.

Gene Symbol	Group	p_adj_NPARC	Diff_meltpoint (°C)
pheS	CBS-Hino	3.58E-07	-14.8
thrC	CBS-Hino	1.28E-02	-10.08
ackA	CBS-Hino	7.41E-05	-5.38
adh	CBS-Hino	4.51E-06	-5.45
adhE	CBS-Hino	3.61E-05	5.22
alaS	CBS-Hino	6.40E-04	-3.17
ald1	CBS-Hino	4.61E-07	-5.74
aldA_1	CBS-Hino	5.19E-04	-5.55
ampA	CBS-Hino	2.30E-02	3.72
arcC1	CBS-Hino	7.64E-03	-3.81
atl	CBS-Hino	8.25E-04	2.54
cdr	CBS-Hino	7.89E-04	2.8
cmk	CBS-Hino	5.54E-05	-4.93
csd	CBS-Hino	2.81E-04	-5.44
cysE	CBS-Hino	8.71E-08	-4.05
dltA	CBS-Hino	2.15E-03	-3.18
entB2	CBS-Hino	2.99E-06	-8.3
fabD	CBS-Hino	2.53E-02	-3.99
femA	CBS-Hino	1.56E-02	-3.28
femB	CBS-Hino	9.07E-05	-4.44
fhs	CBS-Hino	1.13E-05	-5.96
folA	CBS-Hino	2.78E-05	-5.9
folD	CBS-Hino	5.49E-05	-3.7
ftsA	CBS-Hino	5.44E-03	-3
gapC	CBS-Hino	5.39E-04	3.36
gatD	CBS-Hino	1.27E-02	-3.79
gcvPA	CBS-Hino	8.29E-04	3.54
gcvPB	CBS-Hino	3.03E-04	3.04
gcvT	CBS-Hino	1.44E-04	-3.91
gltA	CBS-Hino	1.82E-02	-4.91
glyA	CBS-Hino	2.45E-02	3.63
hemE	CBS-Hino	2.60E-04	-3.05
hemL1	CBS-Hino	3.49E-03	-3.04
hisS	CBS-Hino	7.36E-05	-6.5
ipdC	CBS-Hino	7.55E-09	11.1
ldh2	CBS-Hino	1.07E-05	-6.37
ldhD_2	CBS-Hino	2.79E-03	-4.55
menB	CBS-Hino	6.92E-06	-6.79
merA_1	CBS-Hino	5.96E-03	-3.92
metK	CBS-Hino	2.54E-02	-3.65
miaB_2	CBS-Hino	4.05E-02	-3.01
mqo	CBS-Hino	5.42E-03	-3.14
msrC	CBS-Hino	1.00E-02	-2.84

murF	CBS-Hino	7.54E-03	-4.55
murZ	CBS-Hino	1.80E-03	-4.15
panE	CBS-Hino	6.77E-03	-3
pepT	CBS-Hino	7.73E-03	-3.7
pfkA	CBS-Hino	4.97E-05	2.84
pgk	CBS-Hino	2.15E-04	-3.21
phoP	CBS-Hino	2.95E-05	-2.95
pmi	CBS-Hino	2.64E-03	-3.96
pnbA	CBS-Hino	1.92E-05	-5.42
pyk	CBS-Hino	1.15E-03	-3.83
queF	CBS-Hino	6.23E-03	-6.75
relP	CBS-Hino	2.84E-02	-2.69
rlmL	CBS-Hino	1.46E-02	-3.22
rplN	CBS-Hino	3.84E-02	3.55
rplP	CBS-Hino	2.20E-02	-4.11
RpoA	CBS-Hino	1.08E-02	-2.74
RpoB	CBS-Hino	2.91E-02	-3.22
RpoC	CBS-Hino	4.27E-04	-5.04
rsmG	CBS-Hino	6.88E-05	4.22
sarZ	CBS-Hino	3.19E-02	-3.7
secA1	CBS-Hino	5.83E-03	-4.28
serS	CBS-Hino	1.08E-05	-6.64
treC	CBS-Hino	3.59E-03	-4.52
trmFO	CBS-Hino	2.34E-04	-3.49
trxB	CBS-Hino	4.58E-05	-6.68
typA	CBS-Hino	2.25E-04	-4.52
upp	CBS-Hino	3.73E-03	-5.24
ybeZ	CBS-Hino	2.64E-04	-3.29
ydaG	CBS-Hino	4.22E-07	-6.78
yloU	CBS-Hino	2.09E-04	-3.95
rplB	Hino	4.29E-02	3.73
ackA	Hino	9.45E-03	-3.48
adh	Hino	1.13E-03	-5.75
ampA	Hino	3.24E-04	-9.73
atpA	Hino	4.31E-02	-2.72
cdr	Hino	2.81E-05	2.52
fabI	Hino	7.63E-06	6.61
ftnA	Hino	3.81E-02	-5.4
gap	Hino	9.09E-06	4.22
gcvPB	Hino	3.66E-02	-2.72
glpD	Hino	1.76E-02	-2.82
guaA	Hino	1.18E-05	3.46
gyrA	Hino	1.02E-05	3.93
hsdM	Hino	1.91E-04	3.39
ipdC	Hino	1.96E-08	5.04
mgo	Hino	4.80E-05	2.84

pfkA	Hino	5.08E-09	5.41
pgk	Hino	4.52E-02	-4.2
purB	Hino	5.37E-08	2.99
purD	Hino	4.00E-04	-3.64
rocD	Hino	9.84E-03	-3.49
rplF	Hino	2.17E-05	-10.27
rplM	Hino	3.29E-02	-5.24
rpmC	Hino	2.83E-04	-9.95
rpsC	Hino	5.34E-08	9.33
sucC	Hino	4.93E-03	-2.75
tarJ	Hino	2.18E-06	5.66
yvgN	Hino	8.32E-06	6.55
rlmN	Bi	5.42E-04	7.64
asnS	Bi	1.77E-02	2.71
adh	Bi	1.95E-03	-4.61
dps	Bi	7.45E-06	8.55
mcsB	Bi	4.63E-03	3.58
menB	Bi	3.03E-04	-5.3
yfbR	Bi	3.61E-03	18.85

Table S3. Differentially expressed proteins for *S. aureus* upon the combined CBS and hinokitiol treatment for 0.5, 1, 2 and 4 hours.

Gene Symbol	Time Point (h)	p value	-LOG ₂ (Fold change)
adh	0.5	1.19E-03	-0.31
ahpC	0.5	3.37E-03	-0.29
atl	0.5	5.01E-07	1.26
atpF	0.5	1.77E-02	0.5
codY	0.5	8.76E-03	-0.32
crtP	0.5	1.25E-02	0.55
csbD	0.5	4.41E-03	0.75
csxA	0.5	3.36E-02	0.42
ctpA	0.5	6.77E-03	0.66
dabA	0.5	9.10E-04	0.76
dltD	0.5	2.87E-03	1.05
dnaA	0.5	4.57E-02	0.39
dps	0.5	5.36E-03	-0.34
ebpS	0.5	1.04E-02	0.42
esaA	0.5	3.06E-03	1.23
fadM	0.5	4.90E-03	0.48
fhud2	0.5	2.86E-02	0.45
fib_1	0.5	8.03E-04	1.88
foIE2	0.5	3.31E-02	-0.34
gad	0.5	1.79E-04	1.07
glnA	0.5	7.78E-03	-0.28
gtaB	0.5	4.90E-02	-0.29
hchA	0.5	1.67E-02	-0.29
hflB	0.5	2.49E-02	0.28
hla	0.5	3.72E-02	0.65
ilvA_1	0.5	7.82E-03	-0.38
isaB	0.5	9.51E-03	0.29
ldh2	0.5	5.88E-04	-0.47
ltaS	0.5	2.23E-03	1
lukG	0.5	5.63E-05	1.04
lukH	0.5	6.27E-06	1.19
lytR_1	0.5	2.50E-03	0.84
mecA	0.5	5.43E-07	1.14
metK	0.5	8.17E-03	0.38
mnmA	0.5	3.32E-02	0.52
mnmG	0.5	4.23E-03	0.48
modA	0.5	1.01E-05	1.25
mreC	0.5	2.38E-04	0.98
msrA	0.5	7.13E-03	0.71
msrB	0.5	5.83E-03	-0.29
msrR	0.5	1.32E-02	1.03
murC	0.5	1.38E-03	0.38

murl	0.5	4.01E-03	0.39
opp-1A	0.5	9.16E-04	1.07
oppA	0.5	2.16E-04	1.43
pbp2	0.5	4.91E-03	0.83
pbp3	0.5	1.47E-02	0.84
pbpA	0.5	2.07E-04	0.84
pckA	0.5	4.34E-03	-0.29
prsA	0.5	1.68E-02	0.44
pta	0.5	1.01E-02	-0.29
ptpA	0.5	7.75E-04	0.63
ptsG	0.5	2.66E-02	0.47
qoxA	0.5	5.46E-04	0.44
recA	0.5	3.70E-03	0.29
rlmB	0.5	2.90E-02	0.33
rplE	0.5	4.40E-03	-0.27
rplQ	0.5	4.73E-03	-0.29
rplW	0.5	1.29E-02	-0.27
rplY	0.5	4.06E-02	-0.28
rpmG2	0.5	4.67E-03	0.67
rpmJ	0.5	4.21E-02	1.31
rpsG	0.5	2.61E-03	-0.61
rpsI	0.5	4.43E-02	-0.39
rpsJ	0.5	1.91E-02	-0.44
rpsL	0.5	8.66E-03	0.85
rpsM	0.5	4.57E-02	0.29
rpsP	0.5	1.44E-03	-0.5
rpsS	0.5	1.02E-03	0.71
rpsT	0.5	2.07E-03	-0.34
sbi	0.5	3.19E-06	1.43
sdrD	0.5	1.27E-04	0.68
secA1	0.5	2.43E-03	0.29
secF	0.5	5.44E-03	0.35
sle1	0.5	7.55E-04	0.73
spxA	0.5	9.68E-03	0.34
ssaA	0.5	2.85E-05	1.14
ssaA2_2	0.5	1.89E-02	1.15
ssp	0.5	2.00E-04	1.56
sufC	0.5	2.42E-02	0.3
traD	0.5	7.58E-03	0.48
traG	0.5	2.30E-03	0.98
treB	0.5	2.48E-02	0.35
trxA	0.5	2.30E-04	-0.32
typA	0.5	1.74E-02	0.38
upp	0.5	8.74E-04	-0.27
uppP	0.5	9.99E-03	0.56
uvrB	0.5	5.02E-03	0.55

yclQ	0.5	4.41E-03	0.81
yidA	0.5	1.72E-02	0.6
yrbF	0.5	2.04E-02	0.95
adh	1	3.22E-04	0.51
adk	1	3.00E-03	-0.55
agrA	1	1.75E-02	0.28
ahpC	1	4.40E-03	0.27
aldH	1	7.78E-03	-0.51
amaP	1	5.30E-04	-0.48
arcA	1	1.02E-02	-0.43
argR_2	1	1.89E-03	-0.42
argS	1	4.82E-04	-0.58
asp23	1	1.51E-02	0.28
atl	1	2.61E-04	0.45
bex	1	3.72E-02	-1.01
bsaA_2	1	3.23E-02	-0.34
ccpA	1	1.22E-02	-0.36
chdC	1	4.19E-02	-0.47
citG	1	2.31E-03	-0.46
clpB	1	3.44E-02	-0.26
cmk	1	2.52E-02	0.34
crr	1	4.09E-05	0.43
csd	1	1.83E-03	-0.68
cspA	1	2.78E-02	0.35
ctpA	1	3.83E-02	0.52
cysK	1	1.33E-03	0.31
cysS	1	1.39E-02	-0.54
ddl	1	2.38E-02	-0.55
def	1	6.94E-03	-0.7
dehH1	1	1.37E-02	-0.42
deoC	1	6.06E-03	0.32
dltA	1	2.79E-02	-0.34
dnaA	1	4.72E-02	-0.62
dps	1	2.50E-03	0.73
drm	1	7.06E-02	0.46
drp35	1	1.24E-02	-0.61
ebpS	1	1.19E-02	0.83
eno	1	4.24E-04	0.57
esaA	1	8.45E-03	0.34
fabD	1	3.18E-03	0.56
fabH	1	1.78E-02	-1.04
fabI	1	2.76E-02	-0.43
fda	1	1.16E-04	0.66
fhs	1	3.56E-04	-0.35
fib_1	1	4.48E-04	0.88
floA	1	7.37E-03	-0.31

folA	1	5.88E-03	-0.48
folD	1	1.56E-02	0.36
folE2	1	3.34E-02	0.55
ftnA	1	1.47E-03	0.79
gad	1	4.27E-03	0.99
gatA	1	8.20E-03	-0.64
gatC	1	3.28E-02	0.26
gcvT	1	3.04E-02	0.34
glmS	1	2.24E-02	-0.31
gpsA	1	7.20E-02	-0.86
greA	1	3.87E-03	0.6
gtaB	1	2.54E-02	-0.3
gyrB	1	1.91E-02	-0.34
hemB	1	2.18E-02	-0.31
hemC	1	2.82E-02	-0.35
hemL2	1	9.65E-04	-0.44
hinT	1	1.46E-03	0.63
hla	1	3.55E-02	-0.61
hmp	1	2.27E-02	0.71
hpf	1	6.14E-04	0.61
hprK	1	1.95E-02	-0.57
hpt	1	8.57E-03	-0.31
hsdM	1	7.88E-03	-0.64
hu	1	2.41E-04	0.67
icd	1	2.90E-02	0.38
ileS	1	4.46E-02	-0.6
isaB	1	9.38E-03	0.97
ldh1	1	8.86E-03	-0.29
lepA	1	1.42E-03	-0.41
leuS	1	2.50E-02	-0.83
lipA	1	2.63E-02	-0.69
lukG	1	2.24E-02	0.42
lukH	1	6.43E-04	0.78
lysS	1	1.10E-02	-0.38
lytR_1	1	2.00E-02	-0.41
maeB	1	3.43E-02	-0.31
mecA	1	1.30E-06	0.88
metG	1	1.99E-03	-0.48
metK	1	2.70E-03	-0.72
mhpD	1	8.06E-03	0.31
mlhB_2	1	1.89E-02	0.41
mnmG	1	2.78E-03	-0.57
modA	1	1.84E-04	0.75
mraW	1	2.17E-02	-0.41
msrA	1	6.86E-03	0.79
msrR	1	6.70E-03	-0.72

mtlD	1	2.94E-02	-0.41
murA	1	2.90E-02	-0.47
murB	1	1.07E-02	-0.55
murG	1	1.82E-02	-0.52
murI	1	8.30E-03	0.75
murZ	1	5.70E-02	-0.29
nfo	1	6.69E-03	-0.78
nusG	1	2.28E-02	0.49
obg	1	1.19E-02	-0.43
odhA	1	2.98E-02	-0.36
opp-1A	1	5.37E-03	0.59
opuCa	1	7.98E-04	-0.72
pckA	1	2.63E-03	0.65
pdhB	1	3.07E-02	0.28
pepT_2	1	3.88E-02	-0.44
pfkA	1	5.87E-03	-0.47
pflB	1	1.48E-04	0.39
pgcA	1	8.51E-03	-0.42
pgk	1	1.62E-03	0.53
pgm_2	1	6.29E-03	-0.5
polA	1	2.14E-02	-0.33
prfA	1	2.12E-03	-0.9
proS	1	2.51E-02	-0.39
prsA	1	5.32E-03	0.87
pta	1	5.56E-03	0.45
purB	1	1.13E-02	-0.28
pyc	1	9.35E-03	-0.42
pyrD	1	5.46E-05	-1.07
qoxA	1	6.00E-04	0.66
ribF	1	6.49E-04	-0.56
ribH	1	1.08E-02	-0.66
rlmB	1	8.66E-03	-0.58
rmuC	1	2.27E-02	0.75
rpiA	1	6.13E-02	0.31
rplA	1	4.68E-02	0.61
rplC_1	1	9.79E-03	-0.58
rplJ	1	4.36E-03	0.47
rplP	1	2.34E-02	-0.39
rplQ	1	9.17E-03	-0.3
rplW	1	4.82E-02	0.43
rplX	1	1.24E-02	0.49
rpmD	1	3.76E-02	0.37
rpmF	1	5.07E-02	0.35
rpmG2	1	7.66E-02	0.79
rpoY	1	8.94E-03	0.44
rpsA	1	1.17E-02	0.36

rpsF	1	3.48E-03	0.62
rpsG	1	2.14E-02	0.74
rpsJ	1	1.42E-02	0.7
rpsL	1	5.74E-02	0.7
rpsT	1	5.61E-04	1.61
rsbW	1	1.10E-02	0.46
sarR	1	2.13E-02	0.43
sbi	1	3.87E-03	0.71
scdA	1	2.34E-02	-0.43
sdrD	1	1.35E-02	0.44
sodA	1	9.00E-03	0.82
sodM	1	5.43E-03	0.6
spxA_2	1	2.78E-02	-0.32
ssaA	1	6.53E-03	0.66
ssaA2_2	1	4.09E-02	0.5
ssp	1	1.67E-02	0.57
thiD	1	1.42E-02	-0.42
tig	1	1.51E-03	0.62
tpiA	1	6.66E-03	0.51
trmFO	1	1.46E-04	-0.54
trxA	1	6.15E-05	0.98
tuf	1	5.33E-04	0.49
tyrS	1	6.81E-02	-0.3
valS	1	2.16E-02	-0.33
yehF	1	8.37E-03	-0.55
yhaO	1	2.17E-03	-0.91
yheA	1	7.42E-03	0.53
yloU	1	2.41E-02	0.4
ysdC_2	1	4.88E-03	-0.33
yvgN	1	3.06E-01	0.52
adh	2	6.30E-05	-0.3
arcB	2	1.16E-02	-0.28
artA	2	6.78E-05	0.37
atl	2	4.45E-05	0.58
atpF	2	1.44E-02	-0.41
clpB	2	3.02E-04	-0.59
clpX	2	4.20E-03	-0.4
codY	2	8.43E-04	0.28
def	2	7.03E-04	0.32
dltD	2	1.49E-02	0.34
dps	2	7.14E-04	-0.54
efb	2	1.14E-02	0.57
eno	2	9.75E-03	-0.34
fda	2	5.84E-03	0.3
gad	2	7.06E-03	0.56
gmk	2	1.08E-02	-0.3

greA	2	1.96E-04	0.38
hsdR	2	3.62E-02	-0.3
hu	2	2.19E-03	0.45
isaB	2	1.11E-04	-0.33
lexA	2	7.18E-03	-0.27
lukH	2	4.66E-05	0.68
luxS	2	9.77E-03	0.31
mecA	2	3.01E-03	-0.36
modA	2	3.04E-04	0.72
murB	2	1.50E-02	0.27
nusG	2	3.49E-03	-0.26
pbpA	2	1.46E-02	0.32
plsY	2	1.00E-02	-0.38
pyk	2	1.02E-04	-0.27
pyrH	2	2.01E-03	0.28
rplB	2	1.17E-02	-0.4
rplL	2	2.49E-03	0.29
rplO	2	5.01E-03	0.27
rplP	2	3.84E-03	0.27
rplX	2	5.85E-03	-0.32
rpmF	2	1.08E-03	-0.38
rpsA	2	4.22E-03	-0.29
rpsG	2	9.66E-03	-0.27
rpsK	2	1.17E-03	0.28
rpsS	2	4.15E-03	-0.47
rsbV	2	1.94E-02	0.35
sbi	2	1.64E-04	0.8
sdrD	2	8.52E-05	-0.42
spxA	2	2.10E-02	-0.38
ssp	2	1.63E-04	0.78
tig	2	3.97E-04	0.38
ybeY	2	7.42E-03	-0.27
yrbF	2	3.90E-03	0.64
asp23	4	1.36E-02	0.28
atl	4	3.01E-04	0.3
bsaA_2	4	2.54E-02	0.27
clpB	4	4.11E-04	-0.56
crr	4	2.19E-03	0.33
cspA	4	2.09E-03	0.29
deoC	4	9.40E-03	0.86
dps	4	7.43E-04	-0.58
esxA	4	1.52E-02	0.3
greA	4	1.13E-02	0.31
hla	4	3.07E-02	0.31
lukG	4	1.33E-02	0.24
lukH	4	1.24E-03	0.3

luxS	4	2.53E-03	0.4
mecA	4	1.07E-03	0.32
modA	4	2.44E-02	0.34
murD	4	6.25E-03	0.4
osmC	4	8.56E-03	0.36
pbp2	4	7.14E-03	0.27
pbpA	4	9.53E-04	0.31
psmA4	4	3.50E-03	-0.76
rplB	4	9.23E-03	0.28
rplQ	4	8.08E-03	0.3
rplX	4	2.98E-03	-0.22
rpmF	4	2.11E-03	-0.3
rpmG	4	1.59E-03	0.59
rpsF	4	2.05E-02	0.25
rpsG	4	5.54E-03	-0.33
rpsH	4	1.22E-02	0.22
rpsK	4	1.53E-04	0.34
sarR	4	1.13E-02	0.24
sdrD	4	4.30E-03	0.23
ssp	4	1.03E-02	0.32
tig	4	9.22E-04	0.29
tsf	4	1.43E-03	0.24

Table S4. Primers for qRT-PCR

Knockdown	Forward Primers	Reverse Primers
<i>rpoA</i>	CAGGTGCAGCCGTTAAGTAT	GCGTAACCTCTACCCTTGTTAG
<i>rpoB</i>	GGTATGGCTCGTGATGGTAAA	CTGGAACACTTGGTCTAGAGATG
<i>rpoC</i>	GGAAATCGAAGGTGTCGTAGAA	CAGGACGCTTACGGTGTTTA
<i>eno</i>	AGACGGACTCCAAACAAAGG	CCTGAACGGTGAGAACTACTG
<i>clp</i>	GCGCAATCAGAGAAAAGA	TCCTTGAGCACCACCTAATG
<i>pvlF</i>	GGCTTATCAGGTGGAGGTAATG	ACCTATCCAGTGAAGTTGATTCC
<i>pyk</i>	GTTCAACGGCAGTACTATCT	AACTGATCCACGTCCAATACC
<i>ldh2</i>	GTGGCGACTTAGGAGACATTTA	CCATTGCTTGTTCCGGTTTC
<i>16s</i>	GCGACTTTCTGGTCTGTAAC	GTTTCGCTGCCCTTGTATTG

SI References

- 1 I. Wiegand, K. Hilpert and R. E. Hancock, *Nat. Protoc.*, 2008, **3**, 163-175.
- 2 J. Rappsilber, M. Mann and Y. Ishihama, *Nat. Protoc.*, 2007, **2**, 1896-1906.
- 3 H. Wilkinson, *ggplot2: Elegant Graphics for Data Analysis*, Springer New York, NY, 2009.
- 4 J. Goedhart and M. S. Luisterburg, *Sci. Rep.*, 2020, **10**, 20560.
- 5 D. Szklarczyk, R. Kirsch, M. Koutrouli, K. Nastou, F. Mehryary, R. Hachilif, A. L. Gable, T. Fang, N. T. Doncheva, S. Pyysalo, P. Bork, L. J. Jensen and C. von Mering, *Nucleic Acids Res.*, 2023, **51**, D638-D646.
- 6 P. Shannon, A. Markiel, O. Ozier, N. S. Baliga, J. T. Wang, D. Ramage, N. Amin, B. Schwikowski and T. Ideker, *Genome Res.*, 2003, **13**, 2498-2504.
- 7 N. T. Doncheva, J. H. Morris, J. Gorodkin and L. J. Jensen, *J. Proteome Res.*, 2019, **18**, 623-632.
- 8 D. L. Plubell, P. A. Wilmarth, Y. Zhao, A. M. Fenton, J. Minner, A. P. Reddy, J. Klimek, X. Yang, L. L. David and N. Pamir, *Mol. Cell Proteomics*, 2017, **16**, 873-890.
- 9 Z. Pang, Y. Lu, G. Zhou, F. Hui, L. Xu, C. Viau, Aliya F. Spigelman, Patrick E. MacDonald, David S. Wishart, S. Li and J. Xia, *Nucleic Acids Res.*, 2024, **52**, W398-W406.
- 10 Y. Assenov, F. Ramírez, S.-E. Schelhorn, T. Lengauer and M. Albrecht, *Bioinformatics*, 2008, **24**, 282-284.
- 11 W. Xu, E. Dielubanza, A. Maisel, K. Leung, T. Mustoe, S. Hong and R. Galiano, *Cell Mol. Life. Sci.*, 2021, **78**, 935-947.